journal of the mechanical behavior of biomedical materials 149 (2024) 106235

Contents lists available at ScienceDirect

Journal of the Mechanical Behavior of Biomedical Materials

journal homepage: www.elsevier.com/locate/jmbbm

# Effect of final temperature and heating rate on the mechanical and optical properties of a zirconia veneering ceramic

Andrea Coldea [a], Mustafa Borga Donmez [b,c,*], Bogna Stawarczyk [a]

[a] Department of Prosthetic Dentistry, Dental School, Ludwig-Maximilians-Universität München, Munich, Germany
[b] Department of Prosthodontics, Faculty of Dentistry, Istinye University, Istanbul, Turkey
[c] Department of Reconstructive Dentistry and Gerodontology, School of Dental Medicine, University of Bern, Bern, Switzerland

ARTICLE INFO

*Keywords:*
Veneering ceramic
Firing
Translucency
Shrinkage
Mechanical properties

ABSTRACT

*Purpose:* To evaluate the effect of firing temperature and heating rate on the volumetric shrinkage, translucency, flexural strength, hardness, and fracture toughness of a zirconia veneering ceramic.
*Material and methods:* Zirconia veneering ceramic specimens (N = 45) with varying final temperatures (730 °C, 750 °C, and 770 °C) and heating rates (70 °C/min, 55 °C/min, and 40 °C/min) were fabricated (n = 5). Each specimen's shrinkage, translucency, flexural strength, hardness, and fracture toughness were determined. Two-way analysis of variance, Scheffé test, and Pearson's correlation analysis were used to evaluate data ($\alpha = 0.05$).
*Results:* The shrinkage (44.9 ± 3.1–47.5 ± 1.6 vol%) and flexural strength (74.1 ± 17.4–107.0 ± 27.1 MPa) were not affected by tested parameters ($P \geq 0.288$). The interaction between the main factors affected the translucency, hardness, and fracture toughness of the specimens ($P \leq 0.007$). Specimens with 770 °C final temperature and 70 °C/min heating rate had the lowest (21.8 ± 3.2 %) translucency ($P \leq 0.039$). The hardness ranged between 4.98 ± 0.51 GPa (730 °C; 70 °C/min) and 5.60 ± 0.37 GPa (770 °C; 70 °C/min). Fracture toughness ranged between 0.54 ± 0.04 MPa$\sqrt{m}$ and 0.67 ± 0.08 MPa$\sqrt{m}$ with the highest values for specimens fired at 730 °C with 70 °C/min ($P \leq 0.001$). There was a positive correlation between translucency and hardness ($r = 0.335$, $P = 0.012$), and a negative correlation between fracture toughness and all parameters other than shrinkage (translucency: $r = -0.693/P < 0.001$, flexural strength: $r = -0.258/P = 0.046$, hardness: $r = -0.457/P < 0.001$).
*Conclusions:* Heating rate and final temperature should be considered while fabricating veneered zirconia restorations with tested ceramic as they affected the translucency, hardness, and fracture toughness.

## 1. Introduction

Esthetic demands of patients have increased significantly in recent years and zirconia-based restorations have started to replace metal-fused porcelain restorations (Benetti et al., 2013; Cinar and Altan, 2021). Zirconia is widely preferred due to its superior flexural strength and biocompatibility (Rodrigues et al., 2019). Nevertheless, the inherent opaqueness of zirconia limits its monolithic use (Vichi et al., 2015b), and even though new generations of zirconia offer improved translucency, veneering ceramic is still needed for more pleasing outcomes (Tanaka et al., 2019). Commonly preferred veneering ceramics include feldspathic ceramic, leucite-reinforced ceramic, and fluorapatite ceramic (Sinthuprasirt et al., 2015), while either layering or press-on techniques can be used for veneering (Preis et al., 2013).

Chipping of the ceramic has been the main issue with veneered zirconia restorations (Fischer et al., 2008a, 2008b, 2009; Tholey et al., 2011). Factors such as inadequate bond strength, non-anatomic design of the zirconia framework, and increased veneering ceramic thickness have been attributed to this complication (Lima et al., 2013). However, the firing of the veneering ceramic is also related to chipping as residual tensile stresses associated with the difference in the thermal expansion coefficient between the veneering ceramic and the zirconia framework are generated during cooling (Tanaka et al., 2019). Lower cooling rates and slow cooling processes have been recommended to reduce the residual stresses (Tang et al., 2017; Tholey et al., 2011). However, the heating rate may also affect the internal stresses generated during the firing process (Tan et al., 2012) and unlike the cooling rate (Lima et al.,

* Corresponding author. Department of Reconstructive Dentistry and Gerodontology, School of Dental Medicine, University of Bern, Freiburgstrasse 7, 3010, Bern, Switzerland.
*E-mail address:* mustafa-borga.doenmez@unibe.ch (M.B. Donmez).

https://doi.org/10.1016/j.jmbbm.2023.106235
Received 18 September 2023; Received in revised form 7 November 2023; Accepted 8 November 2023
Available online 11 November 2023

**Abbreviations**

| | |
|---|---|
| Ø | Diameter |
| °C | Celsius |
| a | half of the mean indentation diagonal |
| ANOVA | Analysis of variance |
| c | Half of the mean crack length |
| cm | Centimeter |
| E | Elastic modulus |
| g | Gram |
| GPa | Gigapascal |
| G1 | 770 °C final temperature and 70 °C/min heating rate |
| G2 | 770 °C final temperature and 55 °C/min heating rate |
| G3 | 770 °C final temperature and 40 °C/min heating rate |
| G4 | 750 °C final temperature and 70 °C/min heating rate |
| G5 | 750 °C final temperature and 55 °C/min heating rate |
| G6 | 750 °C final temperature and 40 °C/min heating rate |
| G7 | 730 °C final temperature and 70 °C/min heating rate |
| G8 | 730 °C final temperature and 55 °C/min heating rate |
| G9 | 730 °C final temperature and 40 °C/min heating rate |
| H | Hardness |
| I | Intensity of light |
| $I_0$ | Intensity of monochromatic light |
| $K_{IC}$ | Fracture toughness |
| MPa | Megapascal |
| μm | Micrometer |
| min | Minute |
| mm | Millimeter |
| N | Newton |
| nm | Nanometer |
| r | Radius |
| s | Second |
| S | Shrinkage |
| STL | Standard tessellation language |
| T | Transmission |
| $t_c$ | Transmission coefficient |
| UV/Vis | Ultraviolet–visible |

2013; Meirelles et al., 2016; Preis et al., 2013; Tan et al., 2012; Tanaka et al., 2019; Tang et al., 2017), this aspect of the firing process has not been broadly investigated.

Previous studies have evaluated the effect of thermal treatments such as cooling rate, repeated firings, and annealing on different properties of veneering ceramics (Belli et al., 2013; da Silva Rodrigues et al., 2021; Lima et al., 2013; Longhini et al., 2016; Meirelles et al., 2016; Passos et al., 2017; Preis et al., 2013; Rues et al., 2010; Tang et al., 2017; Vichi et al., 2015a). However, the authors are unaware of a study on the mechanical and optical properties of a zirconia veneering ceramic when different final firing temperatures and heating rates are used. A study based on this topic would be beneficial for clinicians and dental technicians to comprehend the behavior of veneering ceramics as changes in the mechanical and optical properties of veneering ceramics may affect the long-term use of a prosthesis. Therefore, the present study aimed to evaluate the effect of different firing parameters (final temperature and heating rate) on the shrinkage, translucency, flexural strength, hardness, and fracture toughness of a veneering ceramic. The null hypotheses were that the final temperature and heating rate would not affect the i) volumetric shrinkage, ii) translucency, iii) hardness, iv) biaxial flexural strength, and v) fracture toughness of tested veneering ceramic.

## 2. Materials and method

### 2.1. Specimen fabrication

A cylindrical polymer mold (Ø 15 mm × 2 mm) was used to fabricate 45 standardized specimens from a low-fusing veneering ceramic (ceraMotion Zr Transpa, Dentaurum, Ispringen, Germany). For each specimen, approximately 0.8 g of ceramic powder was mixed with 10 drops of corresponding modeling liquid (ceraMotion Modeling Liquid, Dentaurum, Ispringen, Germany) with a glass instrument to form a slurry before the firing process. The slurry was applied to the mold by using a brush and the excess liquid was extracted with a cloth after gentle instrument vibration. The specimen was then removed from the mold and placed on a honeycomb firing tray. The tray was placed 2.5 cm above the firing base of the porcelain furnace (Vacumat 6000M, VITA Zahnfabrik, Bad Säckingen, Germany) with ceramic pins to simulate the position of a crown during firing (Fig. 1). All specimens were produced by a single operator to ensure the standardization of the manual fabrication process and each specimen was fired individually. The cleansing firing of the furnace was performed before starting the fabrication of the specimens in line with the manufacturer's instructions.

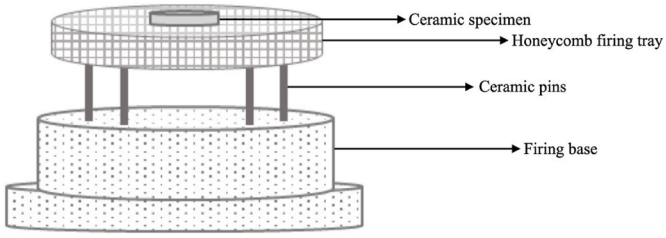


**Fig. 1.** Schematic representation of a specimen before firing.

Specimens were divided into 9 groups (G1-G9) based on the final temperature (730 °C, 750 °C, and 770 °C) and heating rate (2 min (70 °C/min), 6 min (55 °C/min), and 10 min (40 °C/min)) (n = 5) (Fig. 2). The furnace had a standby temperature of 500 °C before the firing cycle of each specimen and every other firing parameter (drying time, holding time, and presence of vacuum) was kept in line with the veneering ceramic manufacturer's instructions (Fig. 2). Regardless of the final temperature and heating rate, all specimens were subjected to fast cooling after firing.

### 2.2. Shrinkage analysis

After fabrication, each specimen was digitized by using a laboratory scanner (Ceramill Map 400, Amann Girrbach, Koblach, Austria) and its corresponding software (Ceramill Mind v2.4, Amann Girrbach, Koblach, Austria) to generate the standard tessellation language (STL) files of the specimens. To facilitate scanning and avoid light scattering from specimens' surfaces, an anti-reflective scan spray (Arti-Spray, Dr. Jean Bausch, Cologne, Germany) was applied on the surface of the specimens before scanning. A customized version of the QualityCheck software (QualityCheck, r2 dei ex machina GmbH, Remchingen, Germany) was used to calculate the volumetric percentage shrinkage of the specimens after green state dimensions (Ø 15 mm × 2 mm) were specified (Fig. 3).

### 2.3. Polishing and translucency analysis

A polishing machine (Abramin, Struers, Ballerup, Denmark) was used to grind the specimens with 40 μm and 20 μm diamond grinding pads (MD Rondo, Struers, Ballerup, Denmark) under constant water irrigation. Then, each specimen was polished to high-gloss with

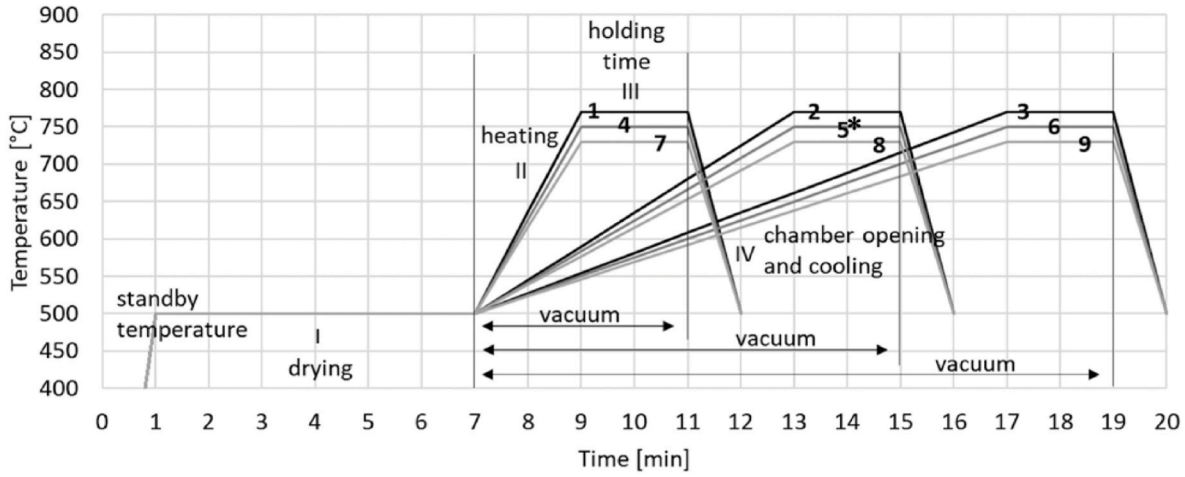


**Fig. 2.** Firing cycles of each test group (G1-G9). *Firing parameters recommended by the manufacturer (control group).

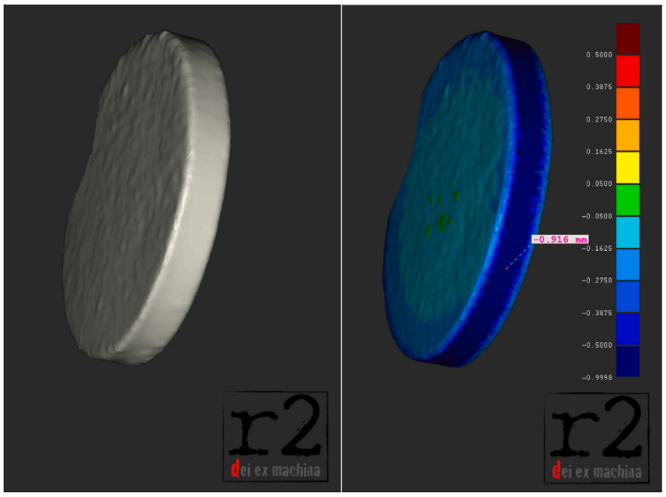

**Fig. 3.** Representative image of shrinkage analysis by evaluating after firing standard tessellation language file of a specimen with green stage dimensions.

polishing pads (MD Largo, Struers, Ballerup, Denmark) and diamond suspensions (DiaPro Largo 3 μm and 9 μm, Struers, Ballerup, Denmark) and ultrasonically cleaned in 96% ethanol (Otto Fischar, Saarbrücken, Germany). After polishing, the specimens had a final diameter of 12 and a final thickness of 1.2 ± 0.05 mm, which were checked with an electronic micrometer (Holex 421490, Hoffmann, Munich, Germany).

Translucency was analyzed by a UV/Vis spectrophotometer (Lambda 35, PerkinElmer LAS, Rodgau, Germany). The specimens were placed in the spectrophotometer at the inlet hole of the integrating Ulbricht sphere. The transmission of light was analyzed for the wavelengths between 400 nm and 700 nm for each specimen. Initial translucency was calculated by the intensity of the monochromatic light $I_0$, and the light I, transmitted through the specimen. The transmission coefficient $t_c$ (%) was calculated by using the equation: $I/I_0 = t_c^x$. The overall light transmission [T] of each specimen was calculated as the integration ($t_c(\lambda)$ $d\lambda$ [$10^{-5}$]) of all $t_c$ values covering the wavelengths from 400 nm to 700 nm. To analyze the light transmission, the T value of each specimen was divided by the T value with no specimen in the spectrophotometer (baseline), to receive light transmission in percentage.

### 2.4. Biaxial flexural strength ($\sigma_f$), hardness (H), and fracture toughness ($K_{IC}$)

A universal testing machine (Zwick 1445, Zwick-Roell, Ulm, Germany) was used to calculate the biaxial flexural strength ($\sigma_f$) of the specimens with a crosshead speed of 1 mm/min. The following formulas were used to calculate the biaxial flexural strength ($\sigma_f$) according to International Organization for Standardization (ISO) standard 6872 (2015):

$$\sigma_f = -0.2387\ P\ (X–Y)/d^2$$

$$X= (1+v)\ In(r_2/r_3)^2 + [(1-v)/2]\ (r_2/r_3)^2$$

$$Y=(1+v)\ [1+In(r_1/r_3)^2] + (1-v)\ (r_1/r_3)^2$$

where $\sigma_f$ is the flexural strength in MPa, P is the fracture load in N, v is the Poisson's ratio (0.19 for veneering ceramics) (Coldea et al., 2015), $r_1$ is the radius of the support circle in mm, $r_2$ is the radius of the loaded area in mm, and $r_3$ is the radius of the specimen in mm.

A universal hardness testing machine (ZHU, Zwick-Roell, Ulm, Germany) was used to measure the hardness of the specimens by applying a load of 49.03 N within 3–5 s and a dwell time of 10 s. Hardness values were measured 3 times for each specimen. Indentation diagonals and crack lengths were measured immediately after indentation by using a light microscope (KVHX-970F, Keyence, Osaka, Japan) under × 300 magnification (Fig. 4).

The hardness was calculated by using the following equation

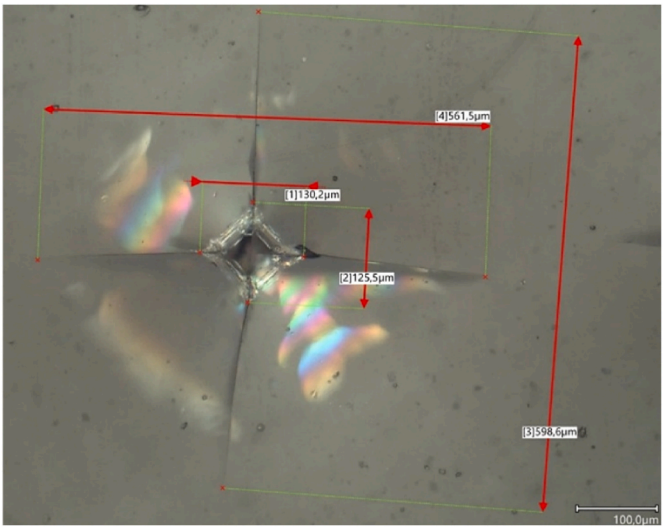


**Fig. 4.** Representative image of a specimen after hardness test showing the Vickers diamond indent and cracks emanating from the indentation. Crack diagonals are approximately 4.5 times larger than the indentation diagonals.

(Sinthuprasirt et al., 2015):

$$H = 1.854(F/d^2)$$

where H is the hardness in MPa, F is the load in N, and d is the mean indentation diagonal length in mm.

The fracture toughness was determined by the following equation (Munz and Fett, 1999):

$$K_{IC} = 0,032 * H * \sqrt{a} * \left(\frac{E}{H}\right)^{\frac{1}{2}} * \left(\frac{c}{a}\right)^{-\frac{3}{2}}$$

where $K_{IC}$ is the fracture toughness in MPa$\sqrt{m}$, H is the hardness in MPa, E is the elastic modulus in MPa (69000 MPa, adapted from (Coldea et al., 2015)), a is the half of the mean indentation diagonal in mm, and c is the half of the mean crack length in mm.

### 2.5. Statistical analysis

The normality of data was assessed by using the Kolmogorov-Smirnov test, which yielded normal distribution for all tested parameters. Therefore, a 2-way analysis of variance followed by a post-hoc Scheffé-test was used to evaluate the data of each parameter with final temperature and heating rate as main factors, and the interaction was also included. The correlation between investigated properties was calculated by Pearson's correlation. All analyses were performed by using a statistical analysis software (SPSS v29, IBM Corp, Armonk, NY, USA) with a significance level of $\alpha = 0.05$.

## 3. Results

### 3.1. Shrinkage results (S)

Final temperature ($P = 0.574$), heating rate ($P = 0.340$), and the interaction between the main factors did not affect the shrinkage of tested low-fusing veneering ceramic ($P = 0.325$). The shrinkage values ranged between 44.9 ± 3.1 vol% (G3, 770 °C; 40 °C/min) and 47.5 ± 1.6 vol% (G5, 750 °C; 55 °C/min) (Table 1).

### 3.2. Translucency results (T)

Fig. 5 presents one specimen from each group for the optical appearance and qualitative analysis of translucency. Specimens were placed on black crosses to visualize translucency and porosity. Figs. 6 and 7 show additional images from groups with distinct features.

The factors final temperature ($\eta_p^2 = 0.988$) and heating rate ($\eta_p^2 = 0.989$), and the interaction between the main factors ($\eta_p^2 = 0.993$) had a significant effect on the translucency of tested low-fusing veneering ceramic ($P < 0.001$). Regardless of the heating rate, the specimens of G7 (730 °C; 70 °C/min) had the lowest translucency (21.8 ± 3.2%) ($P \leq 0.039$). The differences between specimens with 750 °C and 770 °C final temperatures were nonsignificant ($P \geq 0.085$), and translucency values ranged between 79.8 ± 0.2% and 84.1 ± 0.8%. The specimens with 70 °C/min heating rate had the lowest translucency (ranged between 21.8 ± 3.2% and 81.3 ± 0.4%) regardless of the final temperature, while the specimens with 40 °C/min heating rate (83.4 ± 0.2%) had the highest translucency within specimens with 750 °C final temperature ($P < 0.001$) (Table 1, T).

### 3.3. Biaxial flexural strength ($\sigma_f$), hardness (H), and fracture toughness ($K_{IC}$) results

The biaxial flexural strength of tested specimens (ranged between 74.1 ± 17.4 MPa and 107.0 ± 27.1 MPa) was not affected by the interaction between the main factors ($P = 0.470$) or any of the main factors ($P = 0.400$ for final temperature and $P = 0.288$ for heating rate) (Table 1, $\sigma_f$). However, the hardness of the specimens was affected by the interaction between the main factors ($\eta_p^2 = 0.105$, $P = 0.007$) and the final temperature ($\eta_p^2 = 0.176$, $P < 0.001$). Specimens with 770 °C final temperature had higher hardness than those with 730 °C when 70 °C/min (5.60 ± 0.37 GPa) and 55 °C/min (5.42 ± 0.37 GPa) heating rates were used ($P \leq 0.014$). As for the specimens with 40 °C/min heating rate, the specimens with 750 °C final temperature had higher hardness (5.56 ± 0.42 GPa) than those with 730 °C (5.10 ± 0.41 GPa) ($P = 0.006$). Within specimens with 770 °C final temperature, those with 70 °C/min heating rate had higher hardness than those with 40 °C/min heating rate ($P = 0.013$). Heating rate did not affect the hardness of the specimens with 750 °C and 730 °C final temperature ($P \geq 0.061$) (Table 1, H).

Fracture toughness of tested specimens were affected by the interaction between the main factors ($\eta_p^2 = 0.166$) and by both main factors ($\eta_p^2 = 0.121$ for final temperature and $\eta_p^2 = 0.165$ for heating rate) ($P < 0.001$). The specimens with 730 °C final temperature (0.67 MPa$\sqrt{m}$) had the highest fracture toughness within specimens with 70 °C/min heating rate ($P < 0.001$). In addition, the specimens with 70 °C/min heating rate had the highest fracture toughness within specimens with 730 °C final temperature ($P \leq 0.001$) (Table 1, $K_{IC}$). Pearson's correlation analysis showed the positive correlation between translucency and hardness ($r = 0.335$, $P = 0.012$). In addition, fracture toughness had a negative correlation with translucency ($r = -0.693$, $P < 0.001$), biaxial flexural strength ($r = -0.258$, $P = 0.046$), and hardness ($r = -0.457$, $P < 0.001$).

**Table 1**
Descriptive statistics [Mean ± standard deviations (95% confidence intervals)] of tested properties. S: Shrinkage, T: Translucency, σf: Flexural strength, H: Hardness, and $K_{IC}$: Fracture toughness.

| | | | | |
|---|---|---|---|---|
| **770°C** | | **G1** | **G2** | **G3** |
| | S [vol%]: | 47.2 ± 1.1$^{aA}$ (44; 49) | 45.6 ± 2.4$^{aA}$ (41; 49) | 44.9 ± 3.1$^{aA}$ (40; 49) |
| | T [%]: | 81.3 ± 0.4$^{aB}$ (79; 82) | 83.6 ± 0.4$^{bB}$ (82; 85) | 84.1 ± 0.8$^{bB}$ (82; 86) |
| | σf [MPa]: | 98.8 ± 11.5$^{aA}$ (83; 114) | 106.1 ± 29.2$^{aA}$ (68; 143) | 74.1 ± 17.4$^{aA}$ (51; 96) |
| | H [GPa]: | 5.60 ± 0.37$^{bB}$ (5.2; 5.9) | 5.42 ± 0.37$^{abB}$ (5.1; 5.7) | 5.22 ± 0.23$^{aAB}$ (4.9; 5.4) |
| | $K_{IC}$ [MPa$\sqrt{m}$]: | 0.56 ± 0.03$^{aA}$ (0.52; 0.58) | 0.56 ± 0.05$^{aA}$ (0.52; 0.59) | 0.54 ± 0.04$^{aA}$ (0.50; 0.56) |
| **750°C** | | **G4** | **G5** | **G6** |
| | S [vol%]: | 45.8 ± 0.9$^{aA}$ (43; 47) | 47.5 ± 1.6$^{aA}$ (44; 50) | 46.3 ± 2.1$^{aA}$ (42; 49) |
| | T [%]: | 79.8 ± 0.2$^{aB}$ (78; 81) | 82.5 ± 0.3$^{bB}$ (81; 83) | 83.4 ± 0.2$^{cB}$ (82; 84) |
| | σf [MPa]: | 97.8 ± 21.3$^{aA}$ (70; 125) | 107.0 ± 27.1$^{aA}$ (72; 141) | 94.5 ± 23.2$^{aA}$ (64; 124) |
| | H [GPa]: | 5.27 ± 0.30$^{aAB}$ (5.0; 5.5) | 5.27 ± 0.23$^{aAB}$ (5.0; 5.4) | 5.56 ± 0.42$^{bB}$ (5.2; 5.8) |
| | $K_{IC}$ [MPa$\sqrt{m}$]: | 0.59 ± 0.05$^{aA}$ (0.55; 0.62) | 0.56 ± 0.04$^{aA}$ (0.53; 0.59) | 0.57 ± 0.06$^{aA}$ (0.52; 0.61) |
| **730°C** | | **G7** | **G8** | **G9** |
| | S [vol%]: | 45.4 ± 2.3$^{aA}$ (41; 49) | 46.8 ± 1.0$^{aA}$ (44; 48) | 45.4 ± 2.0$^{aA}$ (41; 48) |
| | T [%]: | 21.8 ± 3.2$^{aA}$ (16; 26) | 80.5 ± 1.0$^{bA}$ (78; 82) | 82.1 ± 0.9$^{bA}$ (79; 84) |
| | σf [MPa]: | 87.8 ± 19.0$^{aA}$ (63; 112) | 86.6 ± 24.2$^{aA}$ (55; 117) | 91.1 ± 23.7$^{aA}$ (52; 129) |
| | H [GPa]: | 4.98 ± 0.51$^{aA}$ (4.5; 5.3) | 5.05 ± 0.36$^{aA}$ (4.7; 5.3) | 5.10 ± 0.41$^{aA}$ (4.7; 5.4) |
| | $K_{IC}$ [MPa$\sqrt{m}$]: | 0.67 ± 0.08$^{bB}$ (0.61; 0.72) | 0.56 ± 0.06$^{aA}$ (0.51; 0.59) | 0.56 ± 0.05$^{aA}$ (0.52; 0.60) |
| | | **70 °C/min** | **55 °C/min** | **40 °C/min** |

$^{abc}$: Impact of heating rate within one end temperature; significant differences in rows.
$^{ABC}$: Impact of end temperature within one heating rate; significant differences in columns.

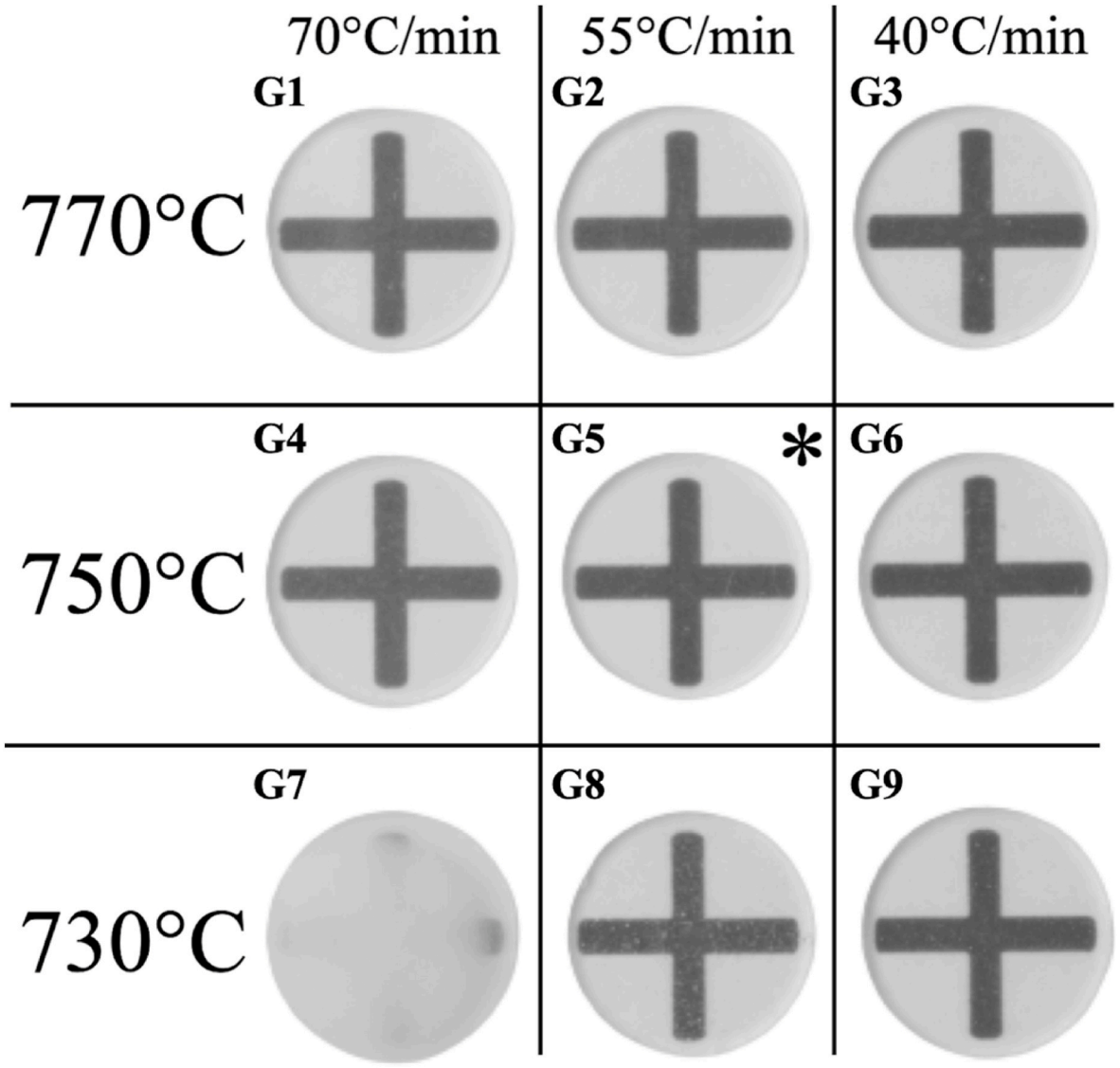


**Fig. 5.** Optical appearance and translucency of one representative specimen from each group fabricated at varying firing parameters (final temperature and heating rate). *Firing parameters recommended by manufacturer.

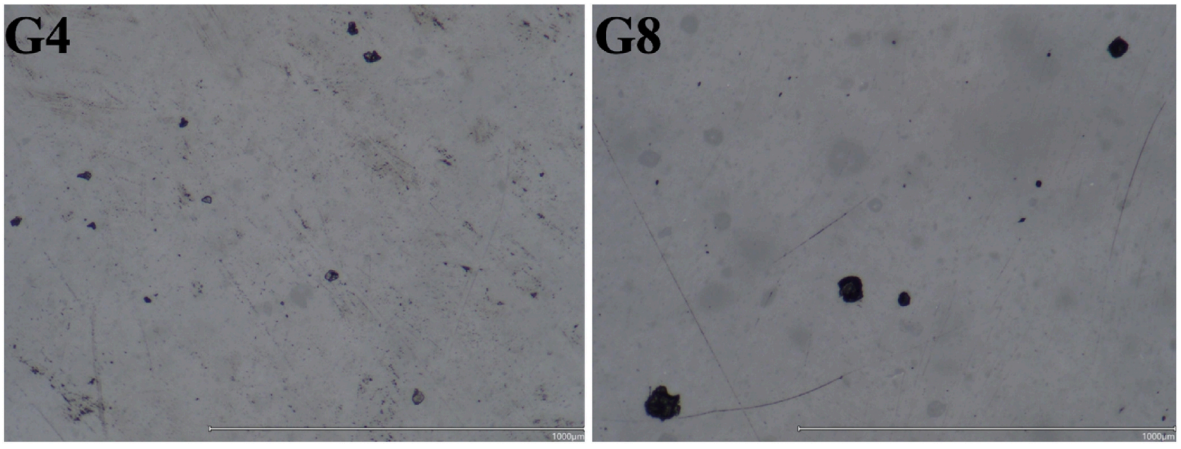


**Fig. 6.** Light microscopy images of G4 and G8 under 200 × magnification. Black spots represent superficial open pores, while greyish spots indicate trapped subsurface pores.

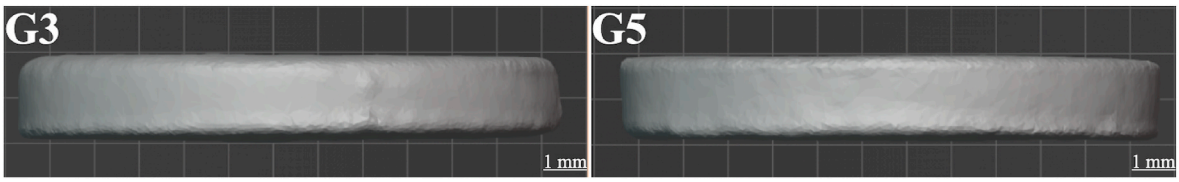


**Fig. 7.** Representative standard tessellation language files of one specimen from G3 and G5 (control) after sintering.

## 4. Discussion

The present study was conducted to evaluate the effect of final temperatures and heating rates that were different than the manufacturer's recommendations on the mechanical and optical properties of a zirconia veneering ceramic. Three final temperatures (730 °C, 750 °C, and 770 °C) and three heating rates (70 °C/min, 55 °C/min, and 40 °C/min) were chosen including manufacturer's parameters as control group. Disk-shaped zirconia veneering ceramic specimens were fabricated without a zirconia framework with 0.8 g of ceramic powder for each specimen to simulate approximately the amount of veneering ceramic used for a crown. Considering that disk-shaped specimens are shorter than an actual crown, the honeycomb-shaped firing tray was elevated with ceramic pins to simulate the positioning of a crown inside the furnace as a recent study has shown that the number of specimens fired in a cycle and their positioning affected their properties (Machado et al., 2021). Standardized test methods for flexural strength and hardness were applied. Non-standardized test methods were employed for volumetric shrinkage, translucency, and fracture toughness. The volumetric shrinkage and biaxial flexural strength of tested low-fusing zirconia veneering ceramic were not affected by the final temperature and heating rate. However, the translucency and fracture toughness of tested veneering ceramic were affected by both the final temperature and heating rate, while its hardness was affected by the final temperature. Therefore, the first and the fourth null hypotheses were accepted, whereas the remaining null hypotheses were rejected.

Considering that the final temperature and heating rate did not affect the volumetric shrinkage and biaxial flexural strength of tested veneering ceramic, it can be hypothesized that these properties may be related to the inherent chemical composition of tested ceramic. However, this speculation needs to be substantiated with studies that involve veneering ceramics with different chemical structures fired by using tested parameters. Considering that the volumetric shrinkage of all specimens was similar, the duration of occlusal and interproximal adjustments needed for those prostheses veneered by using tested ceramic fired under tested parameters may also be similar. However, even if the same framework is used, veneering is operator-related and volumetric shrinkage of a fixed prosthesis could be different than a disk-shaped specimen due to its complex geometric structure. Nevertheless, given that ISO 6872:2015 standard refers to 50 MPa as the threshold value for a ceramic to be used for veneering, tested ceramic could be considered suitable for veneering of a compatible zirconia framework, regardless of the tested final temperature and heating rate. The greatest mean biaxial flexural strength difference among G1, G2, and G3, which was approximately 32 MPa, was higher than those of other groups with the same final temperature. A similar but opposite trend was observed when groups with the same heating rate were evaluated. The greatest mean biaxial flexural strength difference among G1, G4, and G7 was 11 MPa, which was lower than those of other groups with same heating rate. Considering the fact that the specimens were randomly divided into test groups and each specimen was fired individually, the authors think that these differences may be related to the manual fabrication process of the specimens.

Specimens that were fired with the lowest final temperature and the fastest heating rate (G7) had the lowest translucency and hence were opaque, indicating a non-sufficient firing process (Fig. 5). The specimens of G8 and G4 had visible pores with larger pores in G8 (Fig. 6); however, the translucencies of 80.5% and 79.8% respectively were almost in the range of the groups without distinct pores and opacities. Although G3 had optical and mechanical properties comparable to the control G5, they exhibited round edges, indicating overfiring (Fig. 7). Overfiring needs to be considered during veneering, as it changes the shape of the restoration. When pairs with the same final temperature or the same heating rate were evaluated, G6 had higher translucency than G5. However, the authors think that this is a statistical difference related to the number of specimens and could be clinically negligible as the mean translucency difference between G5 and G6 was just 0.9%. In addition, G2 had a mean difference of 1.1% with G5, which was greater than that of G6 and still had no significant differences, which supports the hypothesis on the number of specimens. It should also be mentioned that the greatest mean difference between G5 and the other groups except G7 was 2.7%, which, again, may be clinically perceivable but negligible. Qualitative evaluation of the specimens corroborates these findings as the specimens of G7 had the lowest translucency with a distinct opacity due to light scattering around pores. This is related to underfiring, that is an unfinished melting process of the glassy phase particles within the veneering ceramic. Even though necking between ceramic particles is initiated, they are not fully developed, which leads to pores between particles. In addition, even though pores were somewhat visible on all specimens, they were more evident in G8 and G9. Nevertheless, an apparent difference between G5 and other groups except G7 was not present.

G7, G8, and G9 had hardness that was either similar to or lower than those of other groups, regardless of the heating rate. Due to these significantly or nonsignificantly lower hardness values, the prostheses veneered with tested ceramic fired under the parameters of G7, G8, and G9 might be more prone to wear. Worn areas with increased surface roughness might lead to discoloration, lower fracture resistance, and antagonist wear. When these groups were compared with each other, it can be hypothesized that the specimens of G7 would be more resistant to failure given that it had the highest fracture toughness. Similar to its translucency, lower ceramic particle compaction or necking of the specimens of G7 may be related to the higher fracture toughness due to more tortuous crack paths because of crack deflection around pores. However, considering that enhancing the esthetic appearance of a framework is the initial purpose of veneering and the fact that a negative correlation was observed between the fracture toughness and most of the parameters tested in the present study, significantly higher fracture toughness of G7 may not have a clinical relevance.

The present study was the first on the combined effect of final temperature and heating rate on different properties of a veneering ceramic and significant differences were observed within some of the tested properties. In addition, prior to the actual tests, pilot tests to standardize the effect of final firing temperature and heating rate were performed, given that the specimens were prepared manually. The number of specimens were decided after these tests; however, the absence of a priori power analysis is a limitation of this study. Another limitation was that only one veneering ceramic was tested and all parameters were evaluated without the presence of a zirconia framework. In addition, the specimens were prepared as disks with standardized dimensions to accommodate the tests performed. However, disk-shaped specimens do not reflect actual clinical situations. All specimens were subjected to fast

cooling and even though there is uncertainty regarding the effect of cooling process on mechanical properties of veneering ceramics (Lima et al., 2013; Longhini et al., 2016; Meirelles et al., 2016; Rodrigues et al., 2019, 2021; Tan et al., 2012; Tanaka et al., 2019; Tang et al., 2017), slow cooling may lead to less transient stresses (Benetti et al., 2013) and affect the results. The translucency measurements were performed by using a UV/Vis spectrophotometer and given the diversity of devices that can be used to measure translucency, different devices may lead to different results. The indentation fracture (IF) toughness method was employed to measure the fracture toughness and the IF method was considered applicable, if the crack diagonals exceeded the length of the indentation diagonals by 2.5 (Quinn, 2006). Considering that the crack diagonals measured in this study were approximately 4.5 times larger than the indentation diagonals (Fig. 4), the IF method was applicable. IF method has been used previously to compare the fracture toughness values of different dental ceramics and similar values were reported among ceramics with different chemical compositions (Cesar et al., 2007). Nevertheless, there is no reference fracture toughness value for the tested zirconia veneering ceramic, which was calculated as 0.56 ± 0.04 MPa$\sqrt{m}$, and different methods may affect the measured toughness values (Coldea et al., 2013); therefore, measured fracture toughness values need to be corroborated with additional fracture toughness methods such as single edge V-notched beam. Future studies should elaborate the findings of the present study with different tests and firing temperatures, and also investigate different properties of tested ceramics when veneered over a zirconia framework such as bond strength and long-term resistance to physical stresses caused by thermo-mechanical aging or brushing when fired by using tested parameters to broaden the knowledge on the effect of final temperature and heating rate on the clinical outcomes of veneering ceramics. In addition, the knowledge on how the vertical or horizontal positioning of a prosthesis inside the porcelain furnace affects its properties is limited, and future studies should also focus on this parameter to better standardize the parameters of firing while using veneering ceramics.

## 5. Conclusions

Within the limitations of this in vitro study, the following conclusions could be drawn:

1. Final temperature and heating rate did not affect the volumetric shrinkage and biaxial flexural strength of tested low-fusing zirconia veneering ceramic.
2. Tested veneering ceramic had the lowest translucency and the highest fracture toughness when fired with the lowest final temperature (730 °C) and the fastest heating rate (70 °C/min).
3. The specimens fired with 730 °C final temperature had hardness that was either similar to or lower than those of other specimens.
4. Translucency and hardness of tested veneering ceramic were directly related, whereas its fracture toughness was inversely related to its translucency, biaxial flexural strength, and hardness.

## Funding

This work was part of the IGF Project 21734 N, under the project coordination of AiF Projekt GmbH, Berlin, Germany and financially supported by the BMWK.

## CRediT authorship contribution statement

**Andrea Coldea:** Methodology, Investigation, Data curation, Conceptualization. **Mustafa Borga Donmez:** Writing – original draft. **Bogna Stawarczyk:** Writing – review & editing, Supervision, Formal analysis.

## Declaration of competing interest

The authors declare that they have no known competing financial interests or personal relationships that could have appeared to influence the work reported in this paper.

## Data availability

Data will be made available on request.

## Acknowledgements

The authors thank Dentaurum, VITA Zahnfabrik and HPdent donating material and equipment for this research and r2 dei ex machina GmbH for the shrinkage measurement software.

## References

Belli, R., Frankenberger, R., Appelt, A., Schmitt, J., Baratieri, L.N., Greil, P., Lohbauer, U., 2013. Thermal-induced residual stresses affect the lifetime of zirconia-veneer crowns. Dent. Mater. 29, 181–190.
Benetti, P., Kelly, J.R., Della Bona, A., 2013. Analysis of thermal distributions in veneered zirconia and metal restorations during firing. Dent. Mater. 29, 1166–1172.
Cesar, P.F., Gonzaga, C.C., Miranda Jr., W.G., Yoshimura, H.N., 2007. Effect of ion exchange on hardness and fracture toughness of dental porcelains. J. Biomed. Mater. Res. B Appl. Biomater. 83, 538–545.
Cinar, S., Altan, B., 2021. Effect of veneering and hydrothermal aging on the translucency of newly introduced extra translucent and high translucent zirconia with different thicknesses. BioMed Res. Int. 2021, 7011021.
Coldea, A., Fischer, J., Swain, M.V., Thiel, N., 2015. Damage tolerance of indirect restorative materials (including PICN) after simulated bur adjustments. Dent. Mater. 31, 684–694.
Coldea, A., Swain, M.V., Thiel, N., 2013. In-vitro strength degradation of dental ceramics and novel PICN material by sharp indentation. J. Mech. Behav. Biomed. Mater. 26, 34–42.
da Silva Rodrigues, C., Aurélio, I.L., Fraga, S., da Rosa Kaizer, M., Zhang, Y., May, L.G., 2021. Extended glaze firings for porcelain-veneered zirconia: effects on the mechanical and optical behavior. Dent. Mater. 37, 1096–1106.
Fischer, J., Grohmann, P., Stawarczyk, B., 2008a. Effect of zirconia surface treatments on the shear strength of zirconia/veneering ceramic composites. Dent. Mater. J. 27, 448–454.
Fischer, J., Stawarczyk, B., Hämmerle, C.H., 2008b. Flexural strength of veneering ceramics for zirconia. J. Dent. 36, 316–321.
Fischer, J., Stawarczyk, B., Trottmann, A., Hämmerle, C.H., 2009. Impact of thermal misfit on shear strength of veneering ceramic/zirconia composites. Dent. Mater. 25, 419–423.
International Organization for Standardization, 2015. ISO 6872:2015. Dentistry-Ceramic Materials. International Organization for Standardization, Geneva.
Lima, J.M., Souza, A.C.O., Anami, L.C., Bottino, M.A., Melo, R.M., Souza, R.O., 2013. Effects of thickness, processing technique, and cooling rate protocol on the flexural strength of a bilayer ceramic system. Dent. Mater. 29, 1063–1072.
Longhini, D., Rocha, C.O., Medeiros, I.S., Fonseca, R.G., Adabo, G.L., 2016. Effect of glaze cooling rate on mechanical properties of conventional and pressed porcelain on zirconia. Braz. Dent. J. 27, 524–531.
Machado, P.S., Pereira, G.K.R., da Silva Rodrigues, C., Guilardi, L.F., Valandro, L.F., Rippe, M.P., 2021. Fatigue behavior and colorimetric differences of a porcelain-veneered zirconia: effect of quantity and position of specimens during firing. J. Prosthodont Res. 65, 202–207.
Meirelles, P.D., Spigolon, Y.O., Borba, M., Benetti, P., 2016. Leucite and cooling rate effect on porcelain-zirconia mechanical behavior. Dent. Mater. 32, e382–e388.
Munz, D., Fett, T., 1999. Ceramics: Mechanical Properties, Failure Behaviour, Materials Selection, first ed. Springer Science & Business Media.
Passos, S.P., Linke, B., Major, P.W., Nychka, J.A., 2017. Improving the compatibility of an Y-TZP/porcelain system using a new composite interlayer composition. J. Mech. Behav. Biomed. Mater. 65, 11–19.
Preis, V., Letsch, C., Handel, G., Behr, M., Schneider-Feyrer, S., Rosentritt, M., 2013. Influence of substructure design, veneer application technique, and firing regime on the in vitro performance of molar zirconia crowns. Dent. Mater. 29, e113–e121.
Quinn, G.D., 2006. Fracture toughness of ceramics by the Vickers indentation crack length method: a critical review. CESP 27, 45–62.
Rodrigues, C.D.S., Aurélio, I.L., Fraga, S., Kaizer, M.D.R., Zhang, Y., May, L.G., 2021. Extended glaze firings for porcelain-veneered zirconia: effects on the mechanical and optical behavior. Dent. Mater. 37, 1096–1106.
Rodrigues, C.D.S., Aurélio, I.L., Kaizer, M.D.R., Zhang, Y., May, L.G., 2019. Do thermal treatments affect the mechanical behavior of porcelain-veneered zirconia? A systematic review and meta-analysis. Dent. Mater. 35, 807–817.
Rues, S., Kröger, E., Müller, D., Schmitter, M., 2010. Effect of firing protocols on cohesive failure of all-ceramic crowns. J. Dent. 38, 987–994.
Sinthuprasirt, P., van Noort, R., Moorehead, R., Pollington, S., 2015. Evaluation of a novel multiple phase veneering ceramic. Dent. Mater. 31, 443–452.

Tan, J.P., Sederstrom, D., Polansky, J.R., McLaren, E.A., White, S.N., 2012. The use of slow heating and slow cooling regimens to strengthen porcelain fused to zirconia. J. Prosthet. Dent 107, 163–169.
Tanaka, C.B., Ahmad, N.H.B., Ellakwa, A., Kruzic, J.J., 2019. Effect of cooling protocol on mechanical properties and microstructure of dental veneering ceramics. Dent. Mater. 35, 1498–1505.
Tang, Y.L., Kim, J.H., Shim, J.S., Kim, S., 2017. The effect of different cooling rates and coping thicknesses on the failure load of zirconia-ceramic crowns after fatigue loading. J. Adv. Prosthodont. 9, 152–158.
Tholey, M.J., Swain, M.V., Thiel, N., 2011. Thermal gradients and residual stresses in veneered Y-TZP frameworks. Dent. Mater. 27, 1102–1110.
Vichi, A., Sedda, M., Bonadeo, G., Bosco, M., Barbiera, A., Tsintsadze, N., Carrabba, M., Ferrari, M., 2015a. Effect of repeated firings on flexural strength of veneered zirconia. Dent. Mater. 31, e151–e156.
Vichi, A., Sedda, M., Bonadeo, G., Bosco, M., Barbiera, A., Tsintsadze, N., Carrabba, M., Ferrari, M., 2015b. Effect of repeated firings on flexural strength of veneered zirconia. Dent. Mater. 31, e151–e156.